Measurement of the Effective Nonlinear Parameter Using FWM in Random Polarization Optical Fibers

Nuno A. Silva[1,2], Nelson J. Muga[1,3], and Armando N. Pinto[1,2]

[1]Instituto de Telecomunicações, Universidade de Aveiro, 3810-193 Aveiro, Portugal
Tel: +351234377900, Fax: +351234377901

[2]Departamento de Electrónica, Telecomunicações e Informática, Universidade de Aveiro, 3810-193 Aveiro, Portugal

[3]Departamento de Física, Universidade de Aveiro, 3810-193 Aveiro, Portugal
Emails: nasilva@av.it.pt, muga@av.it.pt, anp@av.it.pt

Fiber-optic parametric amplifiers and optical wavelength convertors based on four-wave mixing (FWM) process in optical fibers are important issues in modern optical communication systems for signal processing applications. In this paper we study theoretically and experimentally the FWM process in optical fibers in a low power regime. We explore the dependence of the FWM efficiency on the relative state of polarization of all optical signals involved in this nonlinear process, to experimentally obtain the transition region between an almost co-polarized situation and a decorrelated state of polarization. Results show the need of considering the polarization dependent effects in the scalar FWM theory in order to obtain an accurate description of this nonlinear process. The 8/9 coefficient for the nonlinear parameter is observed by direct measurement of the optical power of the idler wave, which indicates that the polarization of the optical fields are mostly decorrelated. Results also show that the randomly state of polarization variation in the fiber leads to a loss of efficiency in the FWM process. That loss can be seen as a reduction of the value of the fiber nonlinear parameter.

1. Introduction

The dependence of the fiber index of refraction on the applied electrical field, Kerr effect, gives rise to an intensity-dependent phase shift of the optical field. Four-wave mixing (FWM) is a Kerr nonlinear phenomenon in optical fibers [1]. This phenomenon occurs when light of two or more frequencies (known as pump and signal) are launched into an optical fiber giving rise to a new frequency (known as idler). At the same time that the idler field is created, the signal wave is amplified. This nonlinear process is governed by the third-order nonlinear susceptibility $\chi^{(3)}$ [1]. Efficient generation of the idler wave or amplification of the signal field demands phase-matching condition. In order to achieve that condition, most of the work related with FWM in optical fibers has been done around the fiber zero dispersion, or with the pump and signal wavelength placed very closed [2–4].

Most of the quantum communications protocols requires single or entangled qubits to transmit information between different locations [5]. Recently, single and entangled photon pairs have been used in quantum key distribution experiments in fiber optics,

in order to implement these quantum communications protocols [6, 7].

The FWM process in optical fibers provides a natural way to generate single and entangled photons directly inside a fiber. In this experiments, the FWM process is obtained in a very low power regime [1]. However, the FWM process is highly polarization dependent [8, 9]. In the presence of polarization mode dispersion (PMD) the optical fields involved in this nonlinear process can not maintain their relative state of polarization (SOP). This leads to a loss of efficiency of the FWM process in random polarization optical fibers [8, 9].

In this paper we analyze the generation of the idler wave inside a dispersion shifted fiber through the FWM process in a low power regime. This paper is organized in four sections. In section 2 the experimental setup used to analyze the generation of the idler wave through FWM process in a low power regime is described, and it is presented a theoretical model to describe the FWM process. In section 3 we discuss the polarization dependent effects in the efficiency of the FWM process. Section 4 summarizes the main results presented in this paper.

2. FWM in a Low Power Regime

In Fig. 1 we present a schematic of our experimental setup. This setup was used to analyze the optical power of the idler wave generated through the FWM process in a low power regime.
In the experimental setup, Fig. 1, the pump in continuous mode with wavelength λ_1 passes through a polarization controller (PC), before being coupled to another optical signal λ_2 from a tunable laser source. The signal λ_2 is modulated externally to produce optical pulses with a width at half maximum of approximately 1.6 ns and a repetition rate of 610 kHz. At the modulator output the signal passes from an attenuator which allow us obtain a very low power at the input of the fiber. The two optical fields are launched into a dispersion shift fiber (DSF), with incident powers $P_1(0)$ and $P_2(0)$. The DSF has zero-dispersion wavelength at $\lambda_0 = 1547.34$ nm, length $L = 8865$ m, nonlinear parameter $\gamma = 2.36$ W^{-1}km^{-1}, attenuation, at λ_0, $\alpha = 0.2$ dB/km and dispersion slope $dD_c/d\lambda = 0.069$ ps/(nm^{2}km). Due to the FWM process a new wave, $\lambda_3 = \lambda_1\lambda_2/(2\lambda_2 - \lambda_1)$ is generated inside the optical fiber. At the fiber output a optical filter eliminates the pump and signal waves, while the idler wave, λ_3, passes through the filter and reaches a single photon detector. The single photon detector is based on an APD, operating in the so-called Geiger mode, being $T_g = 2.5$ ns the time during in which the gate of the detector is open. The detector quantum efficiency is $\eta = 10\%$

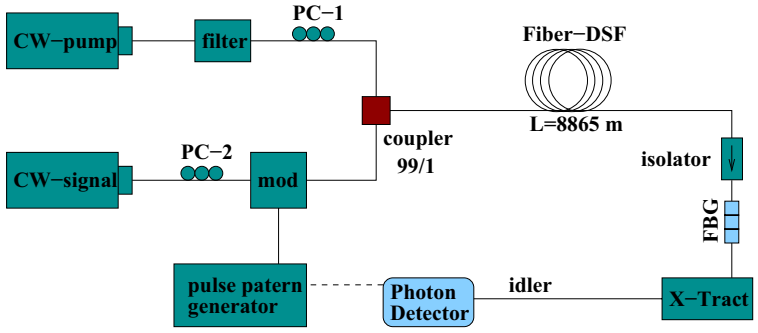

Figure 1: Experimental setup for measuring the optical power generated through FWM in optical fibers in a low power regime. Details of the experimental setup are present in the text.

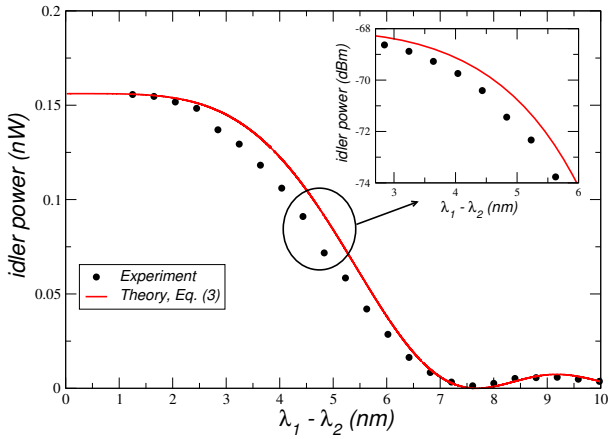

Figure 2: Experimental optical power of the idler wave versus theoretical prediction (3), as a function of wavelength separation between pump and signal fields. We have used: $P_1(0) = 8.71$ mW, $P_2(0) = 1.26 \times 10^{-4}$ mW and $\lambda_1 = 1547.57$ nm.

and the dark count probabilities per gate is $Pr_{dc} = 5 \times 10^{-5}$. The average number of idler photons per pulse that reaches to the single photon detector is given by [10, 11]

$$\langle n \rangle = \frac{1}{\eta} \ln \left(\frac{Pr_{dc} - 1}{Pr_{av} - 1} \right) , \tag{1}$$

where Pr_{av} is the probability of avalanche per gate. The optical power of the idler wave can be obtained using [10]

$$P_m = \frac{\langle n \rangle hc}{\lambda_3 T_g} 10^{\alpha_d/10} , \tag{2}$$

where h is the Planck constant, c is the speed of light in vacuum and α_d is the attenuation, in decibels, from the fiber output to the detector.

2.1 Theoretical Description of the FWM

We assume that all fields involved in the FWM process (pump, signal and idler) remain co-polarized along the propagation in the fiber. In the undepleted-pump approximation the optical power evolution of the idler wave inside an optical fiber in the single pump configuration can be written as [10, 12, 13]

$$P_3(z) = (\gamma P_1(0) z_{eff})^2 P_2(0) \left| \frac{\sin(\kappa z)}{\kappa z} \right|^2 \exp\{-\alpha z\} , \tag{3}$$

where $z_{eff} = (1 - \exp\{-\alpha z\})/\alpha$, and

$$\kappa = \sqrt{\frac{\Delta\beta}{2} \left(\frac{\Delta\beta}{2} + 2\gamma P_1(0) z_{eff}/z \right)} , \tag{4}$$

where

$$\Delta\beta = -\frac{2\pi c \lambda_0^3}{\lambda_1^3 \lambda_2^2} \frac{dD_c}{d\lambda} \bigg|_{\lambda_0} (\lambda_1 - \lambda_0)(\lambda_1 - \lambda_2)^2 , \tag{5}$$

is the phase-matching condition. In Fig. 2 we plot the optical power of the idler wave given by (3) and the experimental data as a function of the wavelength separation between pump and signal fields.
From Fig. 2 we can see that the theoretical model given by (3) does not describe correctly the experimental results for $\lambda_1 - \lambda_2 > 2.8$ nm. That difference is analyzed in section 3.

3. Polarization Effects

In the results presented in Fig. 2, we can see that with the increase of the spectral spacing between pump and signal fields, the optical power of the idler wave measured experimentally is smaller than the theoretical predictions. In the theoretical model it was assumed that the fields remains co-polarized along the propagation in the fiber. However, when the spectral spacing between pump and signal is increased the fields go from an almost co-polarized situation to an decorrelated SOP, which leads to a loss of efficiency in the FWM process [10]. That loss of efficiency can be seen as a reduction of the value of the nonlinear parameter γ [8, 14]. This can be described through a new parameter called effective nonlinear parameter $\gamma_{eff}(\lambda_1, \lambda_2)$, that replaces the γ parameter in (3) [10]. The variation of the effective nonlinear parameter is obtained by fitting the experimental data present in Fig. 2 to (3), with γ replaced by $\gamma_{eff}(\lambda_1, \lambda_2)$. It can be seen in Fig. 3 the evolution of the effective nonlinear parameter with the wavelength separation between pump and signal fields. From Fig. 3 we can see that the $\gamma_{eff}(\lambda_1, \lambda_2)$ is approximately equals to γ for $\lambda_1 - \lambda_2 < 2.8$ nm. This mean that the fields remains almost co-polarized along the evolution in the fiber for small spectral spacings [10]. According with the theory of the Principal States of Polarisation (PSP), exist a small spectral range over which the polarization mode dispersion vector is reasonably constant [15]

$$\Delta\lambda_{psp} \approx \frac{1}{\langle \Delta\tau \rangle}\,, \tag{6}$$

where $\langle \Delta\tau \rangle = 0.362$ ps is the mean differential group delay (DGD) of the fiber. The bandwidth range over which the SOP is reasonably constant is $\Delta\lambda_{psp} \simeq 2.75$ nm, which is in line with the value mentioned above. However, with the increasing separation between pump and signal fields, $\gamma_{eff}(\lambda_1, \lambda_2)$ decreases to $8\gamma/9$, and remains constant for $\lambda_1 - \lambda_2 > 5$ nm [10]. This value for the $\gamma_{eff}(\lambda_1, \lambda_2)$ is in agreement with theoretical predictions for polarization dependent processes [14], which indicates that the pump and signal fields are mostly decorrelated SOP. In Fig. 3 it is also represented the autocorrelation function (ACF) of the PMD vector defined as [16]

$$ACF(\lambda_1, \lambda_2) = e^{-\frac{2\pi c D_p^2 L\left(\frac{1}{\lambda_1} - \frac{1}{\lambda_2}\right)}{3}}\,, \tag{7}$$

where $D_p = 0.132$ ps/$\sqrt{\text{km}}$ is the PMD parameter of the optical fiber. From Fig. 3 we can see that the ACF rapidly decreases with the evolution of $\lambda_1 - \lambda_2$. This mean that the optical fields rapidly evolves from an almost co-polarized situation to a decorrelated SOP [16].
In order to describe analytically the evolution of the $\gamma_{eff}(\lambda_1, \lambda_2)$ with wavelength separation between pump and signal fields we represent that parameter with a hyperbolic secant function given by [10]

$$\gamma_{eff}(\lambda_1, \lambda_2) = \frac{8\gamma}{9} + \frac{\gamma}{9}\text{sech}\left(\frac{(\lambda_1 - \lambda_2)^{A_0}}{T_0}\right)\,, \tag{8}$$

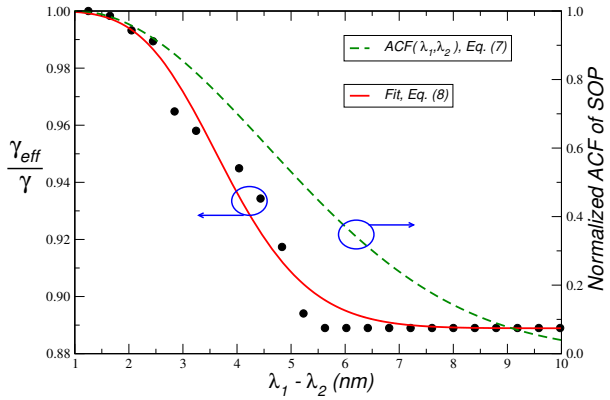

Figure 3: Variation of the $\gamma_{eff}(\lambda_1, \lambda_2)$ parameter with $\lambda_1 - \lambda_2$. In the figure is also represented the normalized ACF of SOP given by (7), and the comparison between the points obtained for the $\gamma_{eff}(\lambda_1, \lambda_2)$ and the fit with and hyperbolic secant function (8).

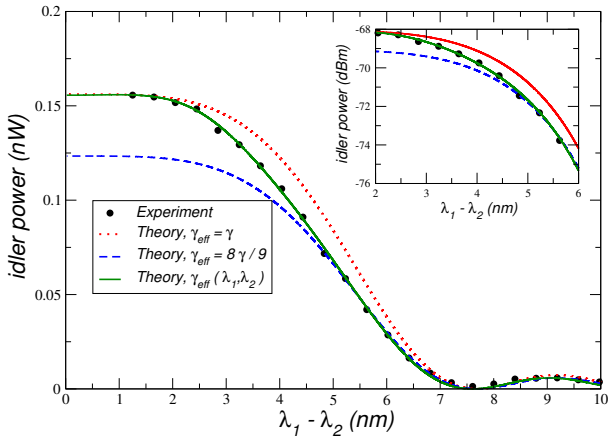

Figure 4: Comparison between the experimental data and the theoretical model given by (3) with γ replaced by (8).

where $A_0 \approx 2.15$ and $T_0 \approx 5.47826 \times 10^{-19}$ are the fitting parameters. The results presented in Fig. 3 also show that the hyperbolic secant describes correctly the variation of the $\gamma_{eff}(\lambda_1, \lambda_2)$ parameter with $\lambda_1 - \lambda_2$ in the transition region 2.8 nm $< \lambda_1 - \lambda_2 <$ 5 nm. In that transition region the optical fields go from an almost co-polarized situation to a decorrelated SOP [10].
Finally, in Fig. 4 we plot the measured optical power of the idler wave and the theoretical model given by (3) with γ replaced by $\gamma_{eff}(\lambda_1, \lambda_2)$, (8), as a function of $\lambda_1 - \lambda_2$. The results presented in Fig. 4 shows a good agreement between the experimental and theoretical data only when γ is replaced by $\gamma_{eff}(\lambda_1, \lambda_2)$, (8).

4. Conclusions

We investigated, both theoretically and experimentally, the FWM process in optical fibers in a low power regime. We show that an accurate description of the FWM in optical fibers can only be obtained by including the polarization dependent effects in the scalar FWM theory. We verify experimentally that the randomly SOP variation in the fiber reduces the optical power of the idler wave. We also show that exist a transition regime where the optical fields go from an almost co-polarized situation to a decorrelated SOP. The 8/9 coefficient for the nonlinear parameter was observed experimentally, when the optical fields evolves with a decorrelated SOP. We introduced

the effective nonlinear parameter, $\gamma_{eff}(\lambda_1, \lambda_2)$ to describe the polarization dependent effects on the generation of the idler wave. Our analysis shows that the $\gamma_{eff}(\lambda_1, \lambda_2)$ varies as an hyperbolic secant with the wavelength separation between the pump and signal fields.

Acknowledgments

This work was partially supported by the Instituto de Telecomunicações under the Laboratório Associado program supported by the Fundação para a Ciência e Tecnologia, FCT, and European Union FEDER program, through the IT/LA projects "QuantTel" and PTDC/EEA-TEL/103402/2008 "QuantPrivTel".

References

[1] G. P. Agrawal, *Nonlinear Fiber Optics*, 3rd ed. San Diego: Academic Press, 2001.

[2] K. Washio, K. Inoue, and S. Kishida, "Efficient large-frequency-shifted three-wave mixing in low dispersion wavelength region in single-mode optical fiber," *Electronic Letters*, vol. 16, no. 17, pp. 658–660, 1980.

[3] K. Inoue, "Four-wave mixing in an optical fiber in the zero-dispersion wavelength region," vol. 10, pp. 1553–1561, 1992.

[4] S. J. Jung, J. Y. Lee, and D. Y. Kim, "Novel phase-matching condition for a four wave mixing experiment in an optical fiber," *Optics Express*, vol. 14, pp. 35–43, 2005.

[5] D. Bouwmeester, A. Ekert, and A. Zeilinger, *The Physics of Quantum Information*. Berlin: Spinger-Verlag, 2000.

[6] P. Antunes, P. S. André, and A. N. Pinto, "Single-photon source by means of four-wave mixing inside a dispersion-shifted optical fiber," in *FIO'06 - Frontiers in Optics*, USA, October 2006.

[7] T. Jennewein, C. Simon, G. Weihs, H. Weinfurter, and A. Zeilinger, "Quantum cryptography with entangled photons," *Physical Review Letters*, vol. 84, no. 20, pp. 4729–4732, 2000.

[8] Q. Lin and G. P. Agrawal, "Effects of polarization-mode dispersion on fiber-based parametric amplification and wavelength conversion," *Optics Letters*, vol. 29, pp. 1114–1116, 2004.

[9] ——, "Effects of polarization-mode dispersion on fiber-based parametric amplification and wavelength conversion," *Optics Letters*, vol. 29, no. 10, pp. 1114–1116, 2004.

[10] N. A. Silva, N. J. Muga, and A. N. Pinto, "Effective nonlinear parameter measurement using FWM in optical fibers in a low power regime," *Quantum Electronics, IEEE Journal of*, vol. 46, no. 3, pp. 285–291, March 2010.

[11] id Quantique, "id 200 single-photon detector module," http://www.idquantique.com/products/files/id200-operating.pdf.

[12] K. Kikuchi and Chaloemphon, "Design of highly efficient four-wave mixing devices using optical fibers," vol. 6, pp. 992–994, 1994.

[13] R. H. Stolen and J. E. Bjorkholm, "Parametric amplification and frequency conversion in optical fibers," vol. 18, no. 7, pp. 1062–1072, 1982.

[14] P. K. A. Wai, C. R. Menyuk, and H. H. Chen, "Stability of solitons in randomly varying birefringent fibers," *Optics Letters*, vol. 16, no. 16, pp. 1231–1233, 1991.

[15] C. D. Poole and R. E. Wagner, "Phenomenological approach to polarisation dispersion in long single-mode fibres," *Electronics Letters*, vol. 22, pp. 1029–1031, 1986.

[16] L. wei Guo and Y. wu Zhou, "Combined effect of pmd and pdl on four-wave-mixing-induced crosstalk in wdm system," *Optics Communications*, vol. 230, no. 4-6, pp. 309 – 312, 2004.